

SI for “Assessing coarse-grained simulation for the analysis of lipid monolayer reflectometry”

A. R. McCluskey,^{1,2,*} J. Grant,³ A. J. Smith,² J. L. Rawle,² D. J. Barlow,⁴ M. J. Lawrence,⁵ S. C. Parker,¹ and K. J. Edler^{1,†}

¹*Department of Chemistry, University of Bath, Claverton Down, Bath, BA2 7AY, UK*

²*Diamond Light Source, Harwell Campus, Didcot, OX11 0DE, UK*

³*Computing Services, University of Bath, Claverton Down, Bath, BA2 7AY, UK*

⁴*Institute of Pharmaceutical Science, King’s College London, London, SE1 9NH, UK*

⁵*Division of Pharmacy and Optometry, University of Manchester, Manchester, M13 9PT, UK*

(Dated: June 24, 2019)

* a.r.mccluskey@bath.ac.uk

† k.edler@bath.ac.uk

This Supplementary Information document is only part of a fully reproducible analysis workflow. The complete workflow, along with all datasets, figure files, and analysis/plotting scripts is available at https://github.com/arm61/sim_vs_trad (DOI: 10.5281/zenodo.2587486) under a CC BY-SA 4.0 license.

S1. ABELÈS MATRIX FORMALISM

The Abelès matrix formalism method invoked the use of the chemically-consistent monolayer model. For this it is necessary to have the scattering length of the individual head and tail components of the different lipid contrasts, these are given in Table SI, while the SLD of the super and subphase were taken as 0 \AA^{-1} and 6.35 \AA^{-1} (for D_2O) and 0 \AA^{-1} (for ACMW) respectively.

TABLE SI. The different scattering lengths of the head and tail lipid components.

| Contrast | d_{13} -DSPC | d_{70} -DSPC | d_{83} -DSPC | h-DSPC |
|---|----------------|----------------|----------------|--------|
| $b_{\text{head}} 10 \times 10^{-4} \text{ \AA}$ | 19.54 | 11.21 | 24.75 | 6.01 |
| $b_{\text{tail}} 10 \times 10^{-4} \text{ \AA}$ | -3.58 | 69.32 | 69.32 | -3.58 |

In order to apply the Abelès matrix formalism, the SLD for the layers, N , were determined as detailed in the text of the paper. This SLD_N allows for the determination of the wavevector, k_N at a particular q -vector in the N -th layer, by considering the difference in SLD between the layer N and the semi-infinite layer 0 (Figure 1),

$$k_N^2 = k_0^2 - 4\pi(\text{SLD}_N - \text{SLD}_0) \quad (\text{S1})$$

where $k_0 = q/2$ and SLD_0 is the SLD of the superphase. For each of the interfaces between two layers, it is possible to evaluate a Fresnel coefficient, $r_{N,N+1}$, which describes the refraction of the probing radiation occurring between the layers N and $N + 1$,

$$r_{N,N+1} = \frac{k_N - k_{N+1}}{k_N + k_{N+1}} \exp(-2k_N k_{N+1} \sigma_{N,N+1}^2). \quad (\text{S2})$$

The exponential factor is due to the fact that the layer is unlikely to be perfectly smooth and will therefore have some roughness, this is modelled as an error function with some width $\sigma_{N,N+1}$ [1]. A phase factor, β_N , which considers the layer thickness, d_N , and the wavevector can then be found,

$$\beta_N = \begin{cases} 0 + 0i & N = 0, \\ k_N d_N & N > 0. \end{cases} \quad (\text{S3})$$

These two parameters are then brought together in the characteristic matrix for the layer, C_N ,

$$C_N = \begin{bmatrix} \exp \beta_N & r_{N,N+1} \exp \beta_N \\ r_{N,N+1} \exp -\beta_N & \exp -\beta_N \end{bmatrix}, \quad (\text{S4})$$

the product sum of which gives a resultant matrix for each value of q ,

$$M(q) = \prod_{n=0}^{n_{\max}} C_N. \quad (\text{S5})$$

From this matrix, the reflected intensity, $R(q)$, can be determined,

$$R(q) = \frac{|M(q)_{21}|}{|M(q)_{11}|}. \quad (\text{S6})$$

S2. MARTINI POTENTIAL MODEL CONSIDERATIONS

It was noted in the work of Koutsoubas [2], that the use of the MARTINI water bead, could result in the ordering of the water structure. This can be observed in the scattering length density profile (Figure S1) when the layer thickness

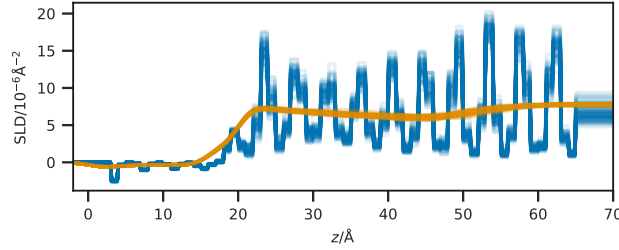


FIG. S1. The scattering length density profile from the MARTINI simulation, at an effective surface pressure of 30 mN m^{-1} with a layer thickness of 1 \AA (blue) and 4 \AA (orange).

TABLE SII. The goodness-of-fit between the calculated and experimental reflectometry profile at a surface pressure of 20 mN m^{-1} .

| Contrast | Monolayer model | Slipid | Berger | MARTINI |
|-----------------------------------|--------------------|---------------------|---------------------|---------------------|
| h-D ₂ O | 59.19 | 167.18 | 130.12 | 210.96 |
| d ₁₃ -ACMW | 119.49 | 125.61 | 120.59 | 160.74 |
| d ₁₃ -D ₂ O | 41.24 | 269.08 | 131.03 | 401.85 |
| d ₇₀ -ACMW | 150.16 | 107.74 | 141.57 | 695.46 |
| d ₇₀ -D ₂ O | 196.96 | 565.22 | 448.13 | 1144.70 |
| d ₈₃ -ACMW | 82.95 | 106.58 | 334.75 | 1127.38 |
| d ₈₃ -D ₂ O | 329.83 | 426.46 | 562.49 | 2780.03 |
| Average \pm Standard deviation | 139.97 ± 92.07 | 252.55 ± 244.41 | 266.95 ± 212.11 | 931.59 ± 852.39 |

of 1 \AA was used. In an effort to reduce this effect, a larger layer thickness, or 4 \AA was used for the MARTINI potential model.

A negative effect of this large layer thickness was that the smoothness associated with the 1 \AA layer was lost. In an effort to reproduce this, an interfacial roughness of 0.4 \AA was included in the model. We believe that this gave the MARTINI potential model a fair chance to reproduce the experimental data. However, as is noted in the main text of the paper, the systematic beading problem leads to more severe issues.

S3. REFLECTOMETRY PROFILES

Figures S2 through S4 show the reflectometry profiles for each of the analysis methods that correspond to surface pressures of 20 mN m^{-1} , 40 mN m^{-1} , and 50 mN m^{-1} . The profile that corresponds to a surface pressure of 30 mN m^{-1} is given in Figure 4. Tables SII through SIV give the χ^2 for each contrast, average χ^2 , and standard deviation for each method at each surface pressure not covered in the main paper.

TABLE SIII. The goodness-of-fit between the calculated and experimental reflectometry profile at a surface pressure of 40 mN m^{-1} .

| Contrast | Monolayer model | Slipid | Berger | MARTINI |
|-----------------------------------|--------------------|---------------------|---------------------|---------------------|
| h-D ₂ O | 50.55 | 195.29 | 113.72 | 302.56 |
| d ₁₃ -ACMW | 61.13 | 68.42 | 42.14 | 107.78 |
| d ₁₃ -D ₂ O | 35.79 | 243.47 | 84.06 | 356.40 |
| d ₇₀ -ACMW | 119.51 | 173.73 | 167.39 | 1484.44 |
| d ₇₀ -D ₂ O | 97.20 | 605.64 | 620.51 | 386.13 |
| d ₈₃ -ACMW | 111.27 | 233.18 | 278.19 | 2334.15 |
| d ₈₃ -D ₂ O | 253.50 | 251.89 | 390.95 | 402.45 |
| Average \pm Standard deviation | 104.13 ± 67.65 | 253.09 ± 213.55 | 242.42 ± 251.81 | 767.70 ± 819.40 |

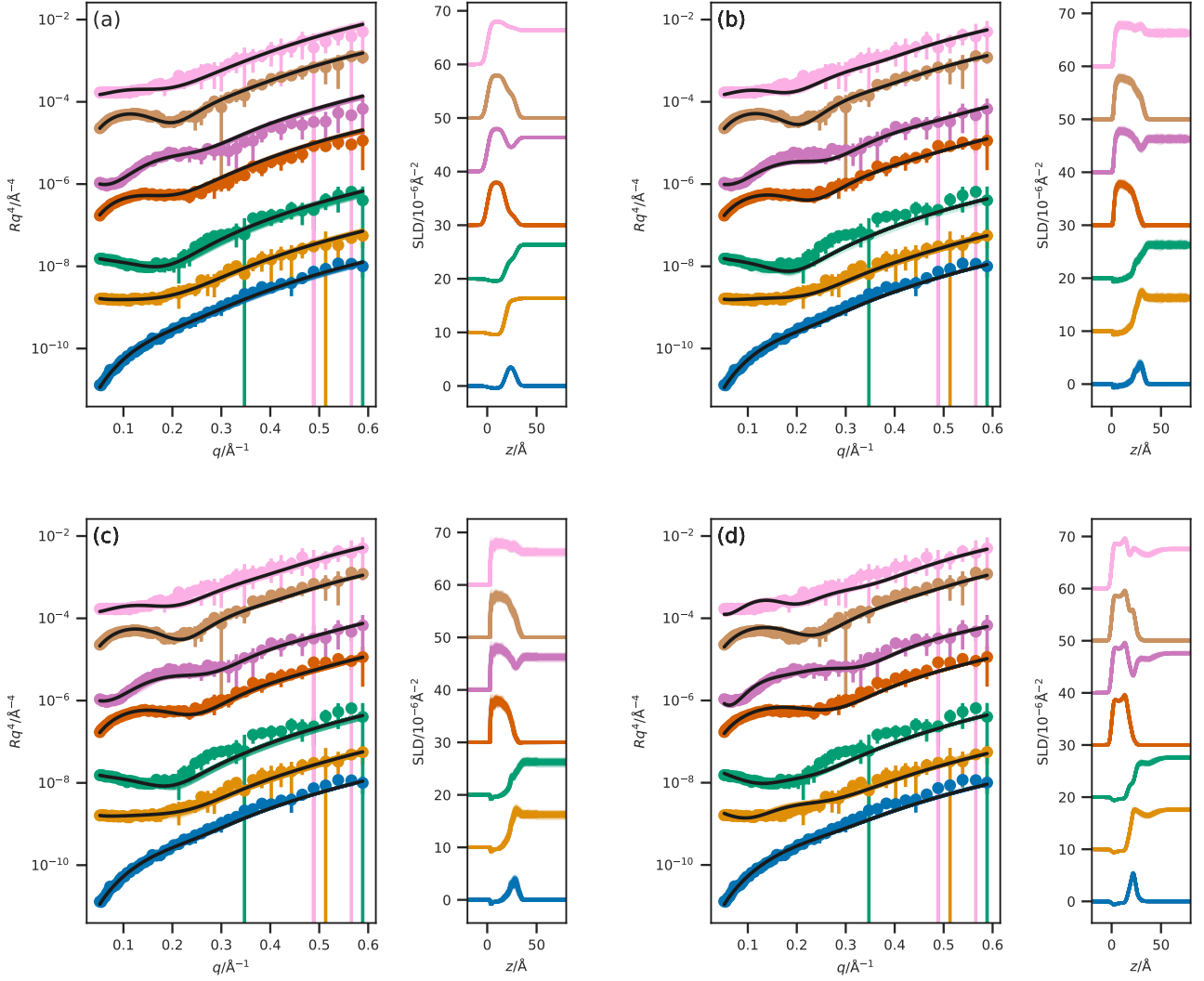


FIG. S2. A comparison of the reflectometry and SLD profiles obtained from (a) the monolayer model, (b) the Slipid simulation, (c) the Berger force-force simulation, and (d) the MARTINI potential model simulation at a surface pressure of 20 mN m^{-1} . From top-to-bottom the contrasts are as follows; d₈₃-D₂O, d₈₃-ACMW, d₇₀-D₂O, d₇₀-ACMW, h-D₂O, d₁₃-D₂O, d₁₃-ACMW. The different contrast reflectometry profiles have been offset in the y -axis by an order of magnitude and the SLD profiles offset in the y -axis by $1 \times 10^{-6}\text{ Å}^{-2}$, for clarity.

TABLE SIV. The goodness-of-fit between the calculated and experimental reflectometry profile at a surface pressure of 50 mN m^{-1} .

| Contrast | Monolayer model | Slipid | Berger | MARTINI |
|-----------------------------------|-------------------|---------------------|---------------------|-----------------------|
| h-D ₂ O | 28.71 | 140.91 | 142.75 | 1301.75 |
| d ₁₃ -ACMW | 103.10 | 47.83 | 28.38 | 278.31 |
| d ₁₃ -D ₂ O | 48.09 | 278.88 | 582.41 | 853.80 |
| d ₇₀ -ACMW | 73.78 | 134.78 | 197.97 | 2958.99 |
| d ₇₀ -D ₂ O | 87.81 | 589.97 | 691.72 | 566.76 |
| d ₈₃ -ACMW | 70.43 | 145.79 | 73.93 | 4240.49 |
| d ₈₃ -D ₂ O | 176.25 | 219.27 | 258.62 | 249.11 |
| Average \pm Standard deviation | 84.03 ± 43.96 | 222.49 ± 206.37 | 282.25 ± 294.50 | 1492.74 ± 1584.60 |

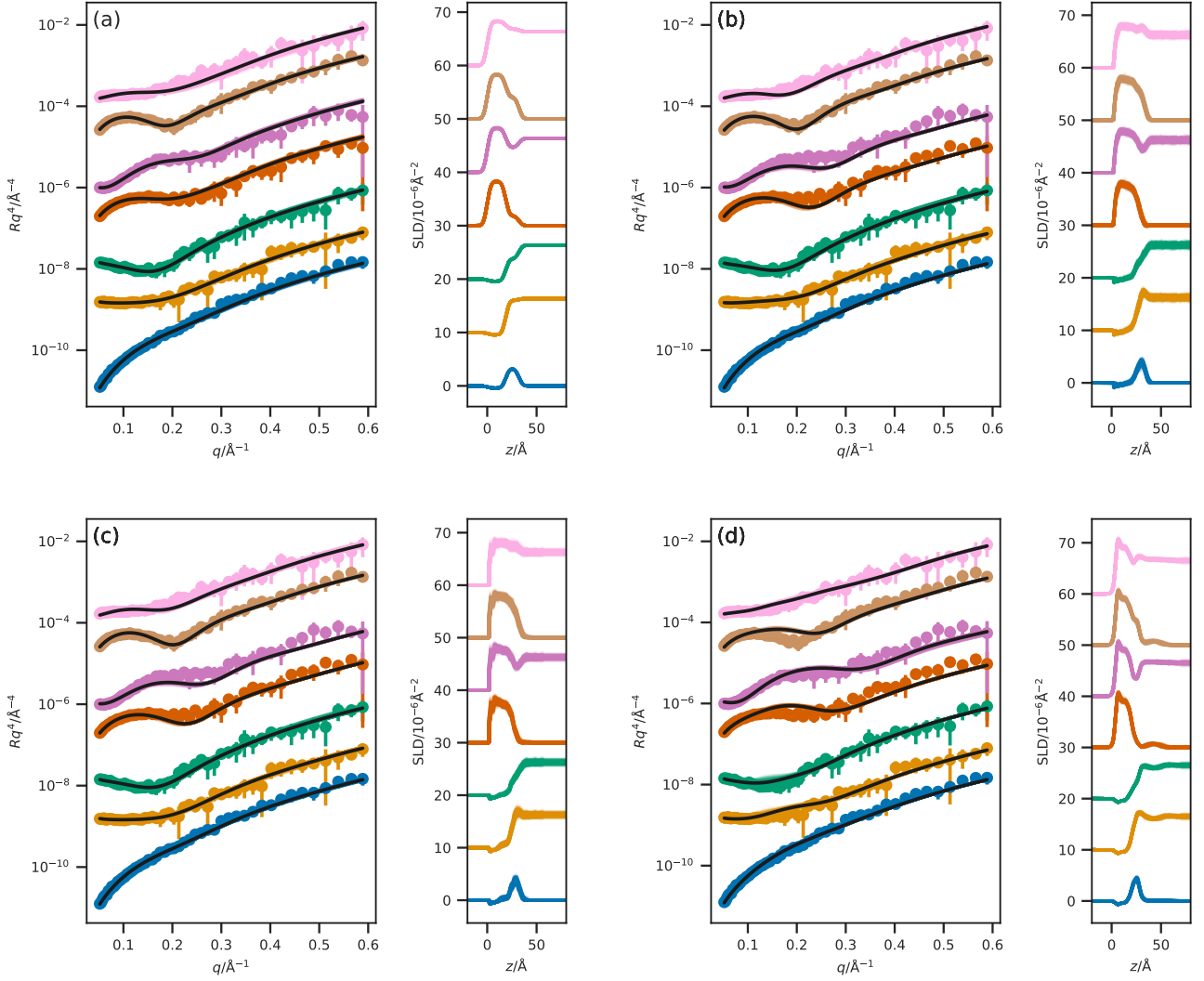


FIG. S3. A comparison of the reflectometry and SLD profiles obtained from (a) the monolayer model, (b) the Slipid simulation, (c) the Berger force-force simulation, and (d) the MARTINI potential model simulation at a surface pressure of 40 mN m^{-1} . From top-to-bottom the contrasts are as follows; $d_{83}\text{-D}_2\text{O}$, $d_{83}\text{-ACMW}$, $d_{70}\text{-D}_2\text{O}$, $d_{70}\text{-ACMW}$, $h\text{-D}_2\text{O}$, $d_{13}\text{-D}_2\text{O}$, $d_{13}\text{-ACMW}$. The different contrast reflectometry profiles have been offset in the y -axis by an order of magnitude and the SLD profiles offset in the y -axis by $1 \times 10^{-6} \text{ \AA}^{-2}$, for clarity.

S4. INTRINSIC SURFACE PLOTS

Figures S5 to S7 show the intrinsic density profiles for water at the air-water interface, for each of the surface pressures not covered in the paper; 20 mN m^{-1} , 40 mN m^{-1} and 50 mN m^{-1} .

S5. QUANTIFICATION OF ROUGHNESS

Tables SV to SVII show the mean, 95 % quantile and spread for the positions of each part of the lipid for each of the surface pressures not covered in the paper; 20 mN m^{-1} , 40 mN m^{-1} and 50 mN m^{-1} .

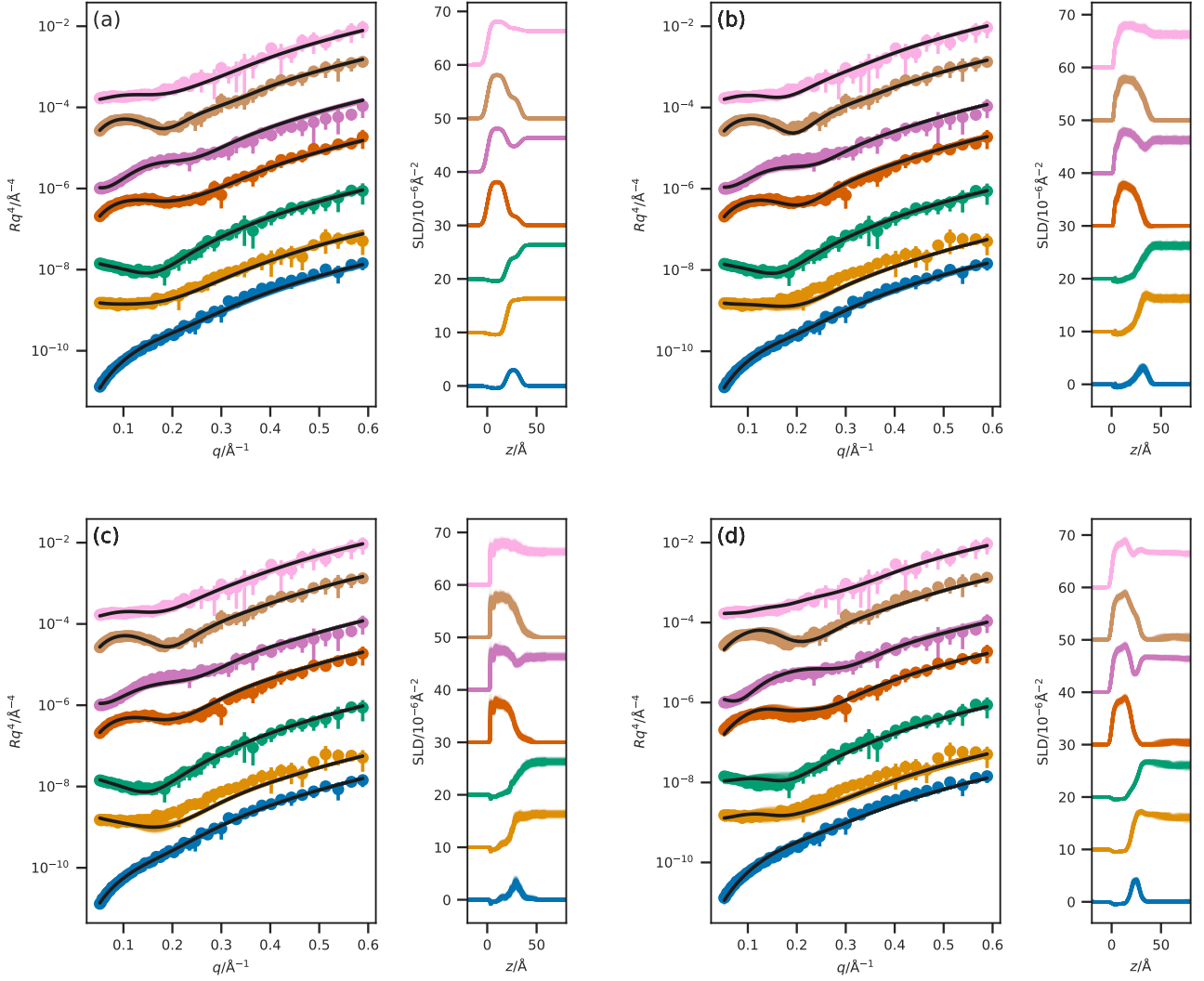


FIG. S4. A comparison of the reflectometry and SLD profiles obtained from (a) the monolayer model, (b) the Slipid simulation, (c) the Berger force-force simulation, and (d) the MARTINI potential model simulation at a surface pressure of 50 mN m^{-1} . From top-to-bottom the contrasts are as follows; $d_{83}-\text{D}_2\text{O}$, $d_{83}-\text{ACMW}$, $d_{70}-\text{D}_2\text{O}$, $d_{70}-\text{ACMW}$, $\text{h}-\text{D}_2\text{O}$, $d_{13}-\text{D}_2\text{O}$, $d_{13}-\text{ACMW}$. The different contrast reflectometry profiles have been offset in the y -axis by an order of magnitude and the SLD profiles offset in the y -axis by $1 \times 10^{-6} \text{ Å}^{-2}$, for clarity.

[1] L. Nérot and P. Croce, Rev. Phys. Appl. (Paris) **15**, 761 (1980).

[2] A. Koutsoubas, J. Phys. Chem. B **120**, 11474 (2016).

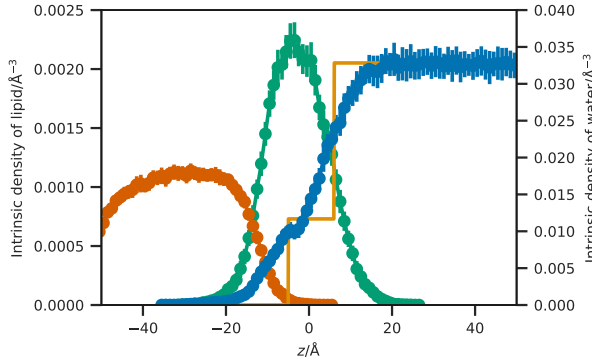


FIG. S5. The simulation time-averaged intrinsic density profile of the water molecules at the interface, where the phosphorus atoms of the lipid heads create the intrinsic surface at $z = 0 \text{ \AA}$ (blue dots), at an APM associated with a surface pressure of 20 mN m^{-1} and the equivalent scattering length density from the chemically-consistent model (orange line).

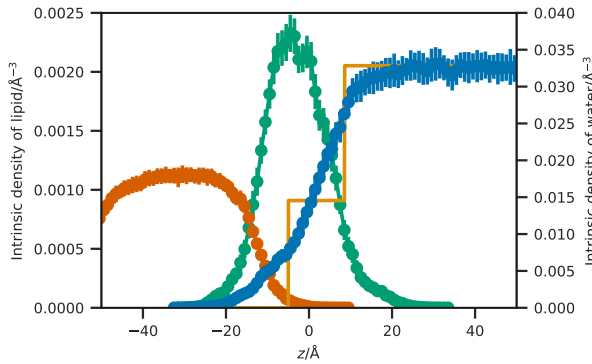


FIG. S6. The simulation time-averaged intrinsic density profile of the water molecules at the interface, where the phosphorus atoms of the lipid heads create the intrinsic surface at $z = 0 \text{ \AA}$ (blue dots), at an APM associated with a surface pressure of 40 mN m^{-1} and the equivalent scattering length density from the chemically-consistent model (orange line).

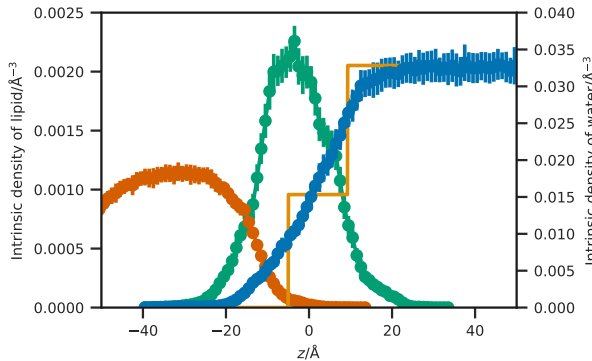


FIG. S7. The simulation time-averaged intrinsic density profile of the water molecules at the interface, where the phosphorus atoms of the lipid heads create the intrinsic surface at $z = 0 \text{ \AA}$ (blue dots), at an APM associated with a surface pressure of 50 mN m^{-1} and the equivalent scattering length density from the chemically-consistent model (orange line).

TABLE SV. The mean, 95 % quantile, and their spread for the position of atoms representative of difference parts of the lipid, at a surface pressure of 20 mN m^{-1} .

| Atom | Mean/ \AA | 95 % quantile/ \AA | Spread/ \AA |
|--------------|--------------------|-----------------------------|----------------------|
| Start-Head | 64.2 | 73.7 | 9.5 |
| Mid-Head | 65.1 | 74.2 | 9.1 |
| End-Head | 68.2 | 77.2 | 9.0 |
| Start-Tail 1 | 69.4 | 78.0 | 8.5 |
| Start-Tail 2 | 70.4 | 79.3 | 8.8 |
| Mid-Tail 1 | 78.3 | 84.0 | 5.8 |
| Mid-Tail 2 | 79.6 | 85.6 | 6.0 |
| End-Tail 1 | 88.5 | 90.5 | 2.1 |
| End-Tail 2 | 89.6 | 90.7 | 1.1 |

TABLE SVI. The mean, 95 % quantile, and their spread for the position of atoms representative of difference parts of the lipid, at a surface pressure of 40 mN m^{-1} .

| Atom | Mean/ \AA | 95 % quantile/ \AA | Spread/ \AA |
|--------------|--------------------|-----------------------------|----------------------|
| Start-Head | 69.4 | 78.6 | 9.2 |
| Mid-Head | 70.3 | 79.8 | 9.5 |
| End-Head | 73.5 | 82.8 | 9.4 |
| Start-Tail 1 | 74.7 | 83.6 | 8.9 |
| Start-Tail 2 | 75.9 | 85.0 | 9.1 |
| Mid-Tail 1 | 83.7 | 89.6 | 5.9 |
| Mid-Tail 2 | 85.3 | 91.9 | 6.6 |
| End-Tail 1 | 94.2 | 96.9 | 2.7 |
| End-Tail 2 | 95.6 | 97.1 | 1.5 |

TABLE SVII. The mean, 95 % quantile, and their spread for the position of atoms representative of difference parts of the lipid, at a surface pressure of 50 mN m^{-1} .

| Atom | Mean/ \AA | 95 % quantile/ \AA | Spread/ \AA |
|--------------|--------------------|-----------------------------|----------------------|
| Start-Head | 71.3 | 83.2 | 11.9 |
| Mid-Head | 72.6 | 83.9 | 11.2 |
| End-Head | 75.6 | 86.8 | 11.2 |
| Start-Tail 1 | 76.7 | 87.8 | 11.1 |
| Start-Tail 2 | 77.9 | 89.0 | 11.1 |
| Mid-Tail 1 | 85.4 | 94.8 | 9.4 |
| Mid-Tail 2 | 87.3 | 96.4 | 9.1 |
| End-Tail 1 | 95.8 | 100.3 | 4.5 |
| End-Tail 2 | 97.6 | 100.4 | 2.9 |